Electrostatic Operation and Curvature Modeling for a MEMS Flexible Film Actuator *

B. Edmonds, Jr.[1], J. Ernstberger[2], K. Ghosh[3], J. Malaugh[4], D. Nfodjo[5], W. Samyono[6], X. Xu[7]
and
D. Dausch[8], S. Goodwin[9], R.C. Smith[10, †]

[1]Department of Mathematics, Virginia Commonwealth University, Richmond, VA 23284
[2,10]Center for Research in Scientific Comp., North Carolina State Univ., Raleigh, NC 27695
[3]Department of Computer Science, University of Wisconsin-Milwaukee, Milwaukee, WI 53201
[4]Department of Mathematics, University of Alabama at Birmingham, Birmingham, AL 35294
[5]Deparment of Mathematics, University of Louisville, Louisville, KY 40292
[6]Department of Mathematics and Statistics, Old Dominion University, Norfolk, VA 23529
[7]Department of Mathematics, Florida State University, Tallahassee, FL 32306
[8,9]MCNC Research and Development Institute, Research Triangle Park, NC 27709

Abstract

In this paper we develop a mathematical model to simulate the actuation of a multilayer metallic strip. In the first step of the model development, we employ the theory of Judy [4] and Timoshenko [5] to quantify the radius of curvature in the unimorph due to differing thermal coefficients in the constituent materials. The resulting radius of curvature is subsequently used to compute the voltage required to uncurl the actuator. Numerical experiments were performed with the model and the trends were found to be in agreement with experimental data.

1 Introduction and Motivation

The electrostatic flexible film actuator, also known as an "Artificial Eyelid," is a unique MEMS (MicroElectronic Mechanical System) actuator fabricated from polyimide and thin metal films which provide high mechanical displacement (100's of microns) and high operational frequency (>5 kHz). The device is comprised of a polyimide/Au/polyimide structure in the flexible film portion of the actuator and a metal or transparent electrode on the substrate (Si, quartz, sapphire, etc.) surface. Actuation of the device is achieved by applying a voltage between the electrode in the flexible film and the electrode on the substrate, causing the flexible film to flatten or uncurl across the substrate surface due to electrostatic attraction. When the voltage is removed, the actuator recoils to its curled state. Applications of this device include optical shutters, electrical switches and microfluidic valves.

A sacrificial release layer film is deposited between the flexible film and the substrate is etched away after forming the flexible film portion. Due to stresses in the films caused by thermal expansion mismatch during the polyimide cure at 410 ^{o}C, removal of the release film causes the flexible film portion of the actuator to curl. The degree of curl can be altered by changing the thicknesses of the flexible film constituents, and the electrostatic operating voltage is dependent on the radius of curvature (and thus stress) of the film. Actuators with tight

*This problem was investigated by the first seven authors under the direction of the last three authors during the Industrial Mathematical and Statistical Modeling Workshop for Graduate Students held at North Carolina State University on July 21–July 29, 2003.

†Corresponding author: rsmith@eos.ncsu.edu, (919) 515-7552

curl have operating voltage in the range of 220-340 V, whereas actuators with less curl operate in the range of 100-180 V.

The objective of this investigation is to develop a baseline characterization method for determining the expected operating voltage for a given radius of curvature or film stress. The assumption is that the thermal stresses causing the film to curl must be overcome by the electrostatic force in order to uncurl the actuator. This provides a threshold voltage where the actuator begins to uncurl. Concurrently, we confirm our method for determining the radius of curvature expected in the actuator based on film thicknesses and mechanical properties. We currently perform calculations based on the mathematical model proposed by Judy [4] and Timoshenko [5]. The current calculation provides reasonably accurate trends, but further optimization is needed in the model.

2 Modeling Issues to Predict Curvature and Displacement as Functions of Material Proportion

The different actuator models are constructed using appropriate mathematical relations to predict curvature and displacement as functions of material thickness. The model used for actuator simulation is quantified using characteristics of the material and temperature. Experiments were carried out to evaluate the variation of the thickness of the top layer of the multilayer strip with the radius of curvature of the actuator. The mathematical model for the actuator, used for computing the operating voltages for various dimensions of the radius of curvature of the actuator, is described by Judy [4] as

$$\frac{\sigma_1}{E_1} + \frac{P_1}{E_1 a_1 b} + \frac{a_1}{2\rho} = \frac{\sigma_2}{E_2} - \frac{P_2}{E_2 a_2 b} - \frac{a_2}{2\rho} \tag{1}$$

where a_1 and a_2 are the thicknesses of the layer, from top to bottom, E_1 and E_2 denote the respective Young's moduli, and b is the width of the strip. We also consider the ratios

$$m = \frac{E_1}{E_2}, n = \frac{a_1}{a_2}.$$

The equation gives an insight into the radius of curvature with respect to thickness of the material of the topmost layer. The force required to uncurl the actuator is calculated from the radius of curvature specified by the model. Hence the electrostatic voltage can be computed to uncurl the actuator.

2.1 Two-Layer Case

The model of the two-layer case was developed by using the models of Judy [4] and Timoshenko [5]. Both authors describe the motion of small cantilevers (Timoshenko in relation to thermostats). Although the films that are discussed in this paper have notably different properties, the two previously mentioned papers make note of properties that also apply to this problem.

The model summarizes the forces placed on the bi-metal strip and can be applied to the films given different Young's moduli E_i, residual stresses σ_i, axial force P (since it is assumed that although there are two axial forces, in a two-layer case they are the same), and the force due to curvature (ρ).

Combining the methods used in [4, 5], we propose a new model to compute the radius of the actuator:

$$\alpha_1 \Delta T + \frac{\sigma_1}{E_1} + \frac{P_1}{E_1 a_1 b} + \frac{a_1}{2\rho} = \alpha_2 \Delta T + \frac{\sigma_2}{E_2} - \frac{P_2}{E_2 a_2 b} - \frac{a_2}{2\rho}. \tag{2}$$

Here α is the corresponding coefficient of expansion for each layer of the film and ΔT is the change in temperature of the respective layer. Note that a_i is the thickness of the strip and that b is the width of the strip (which Timoshenko takes as unity).

With manipulation the force due to curvature (ρ) can be found to be

$$\frac{1}{\rho} = \frac{(\alpha_2 - \alpha_1)\,\Delta T - \frac{\sigma_1}{E_1} + \frac{\sigma_2}{E_2}}{\frac{a_1+a_2}{2} + 2\left(\frac{E_1 a_1^3 - E_2 a_2^3}{12}\right)\left(\frac{1}{E_1 a_1} - \frac{1}{E_2 a_2}\right)}. \tag{3}$$

2.2 Three-Layer Case and Five-Layer Case

For the previous two-layer case, we had seen that Judy [4] and Timoshenko [5] give models and examples. However, the three-layer case depicted in Figure 1 is similar in nature and is modeled on the assumptions similar to that of two-layered case. The relation for the axial stress P_i given by

$$P_1 - P_2 - P_3 = 0. \tag{4}$$

Going through P_1, the sum of the moments is given by

$$m_1 + m_2 + m_3 = P_2\left(\frac{a_2}{2} + \frac{a_1}{2}\right) + P_3\left(\frac{a_3}{2} + a_2 + \frac{a_1}{2}\right). \tag{5}$$

The relationship established between ρ and the moment m_i for each i from one to three is

$$m_1 = \frac{E_1 I_1}{\rho}, m_2 = \frac{E_2 I_2}{\rho}, m_3 = \frac{E_3 I_3}{\rho}.$$

There is (similar to the two-layer case) a relationship made between the stresses between the first and second layers and the second and third layers.

$$\alpha_1 \Delta T + \frac{\sigma_1}{E_1} + \frac{P_1}{E_1 a_1 b} + \frac{a_1}{2\rho} = \alpha_2 \Delta T + \frac{\sigma_2}{E_2} - \frac{P_2}{E_2 a_2 b} - \frac{a_2}{2\rho} \tag{6}$$

$$\alpha_2 \Delta T + \frac{\sigma_2}{E_2} - \frac{P_2}{E_2 a_2 b} + \frac{a_2}{2\rho} = \alpha_3 \Delta T + \frac{\sigma_3}{E_3} - \frac{P_3}{E_3 a_3 b} - \frac{a_3}{2\rho}. \tag{7}$$

Finally, the connection between ρ and the axial stresses P_i can be expressed as

$$\frac{E_1 I_1 + E_2 I_2 + E_3 I_3}{\rho} = P_2\left(\frac{a_2}{2} + \frac{a_1}{2}\right) + P_3\left(\frac{a_3}{2} + a_2 + \frac{a_1}{2}\right). \tag{8}$$

Simplifying the system of equations for ρ yields

$$\frac{1}{\rho} = \frac{z}{y + \frac{a_2 + a_3}{2}} \tag{9}$$

where

$$z = x - \Delta T\left(\alpha_2 - \alpha_3\right) + \frac{\sigma_3}{E_3} - \frac{\sigma_2}{E_2} \tag{10}$$

$$x = \frac{\sigma_2 a_2}{E_2 a_2} + \frac{a_1 + a_2}{E_3 a_3\left(a_3 + a_1 + 2a_2\right)} \tag{11}$$

$$y = 2\frac{E_1 I_1 + E_2 I_2 + E_3 I_3}{E_3 b a_3 (a_3 + a_1 + 2a_2)}. \tag{12}$$

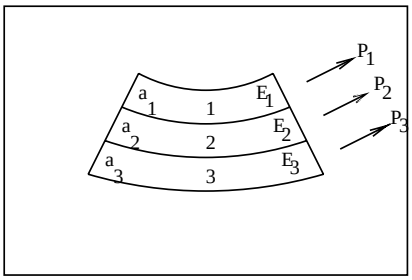

Figure 1: Three-layer film with respective Young's moduli, thicknesses, and thermal conductivity coefficients.

The five-layer case depicted in Figure 2 is a direct extension from the three-layered case in that two layers of chromium were added around the original gold-conducting layer. The basic equation to build the model is

$$P_1 - P_2 - P_3 - P_4 - P_5 = 0. \tag{13}$$

Going through P_1, the sum of the moments is given as

$$\begin{aligned} m_1 + m_2 + m_3 + m_4 + m_5 &= P_2\left(\frac{a_2}{2} + \frac{a_1}{2}\right) + P_3\left(\frac{a_3}{2} + a_2 + \frac{a_1}{2}\right) \\ &+ P_4\left(\frac{a_4}{2} + a_3 + a_2 + \frac{a_1}{2}\right) + P_5\left(\frac{a_5}{2} + a_4 + a_3 + a_2 + \frac{a_1}{2}\right). \end{aligned} \tag{14}$$

The moments, m_j, are once again given by

$$m_j = \frac{E_j I_j}{\rho} \text{ for } j = 1, \ldots, 5. \tag{15}$$

After following the mathematical steps in deriving the relationships and the layers in the three layered case, the relation between the $E_j I_j$'s and ρ are

$$\frac{\sum_{j=1}^{5} E_j I_j}{\rho} = \frac{EI}{\rho} = \sum_{k=2}^{5} P_k L_k \tag{16}$$

where the L_i's are denoted by

$$L_2 = \frac{a_2}{2} + \frac{a_1}{2} \tag{17}$$

$$L_3 = \frac{a_3}{2} + a_2 + \frac{a_1}{2} \tag{18}$$

$$L_4 = \frac{a_4}{2} + a_3 + a_2 + \frac{a_1}{2} \tag{19}$$

$$L_5 = \frac{a_5}{2} + a_4 + a_3 + a_2 + \frac{a_1}{2}. \tag{20}$$

Through analysis similar to that for the two and three-layered cases, ρ is specified by

$$\frac{1}{\rho} = \frac{(M+N)}{\frac{a_3+a_2}{2} - \frac{EI}{L_2 E_2 a_2 b}} \tag{21}$$

where

$$M = \alpha_3 \Delta T + \frac{\sigma_3}{E_3} - \frac{P_3}{E_3 a_3 b} + \frac{L_3}{L_2 E_2 a_2 b} + \frac{L_4 E_4 a_4}{L_2 E_3 a_3 E_2 a_2 b} + \frac{L_5 E_5 a_5}{L_2 E_2 E_3 a_2 a_3 b} \tag{22}$$

$$N = -\alpha_2 \Delta T - \frac{\sigma_2}{E_2} - \frac{L_4 k}{L_2 E_2 a_2 b} - \frac{L_5 q}{L_2 E_2 a_2} \tag{23}$$

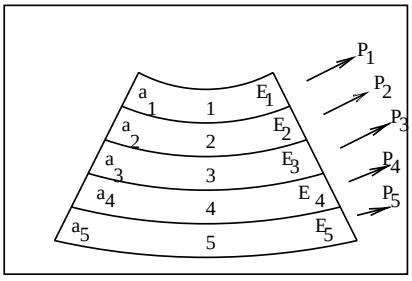

Figure 2: Five-layer varies from the three-layer case in that two chromium layers surround the inner gold conducting layer.

and

$$k \quad + \quad \frac{P_3 E_4 a_4}{E_3 a_3} = P_4, \tag{24}$$

$$q \quad + \quad \frac{\left(k + \frac{P_3 E_4 a_4}{E_3 a_3}\right) E_5 a_5}{E_4 a_4} = P_5. \tag{25}$$

The system of equations is solved using a line search Newton Method.

3 Modeling Of Electrostatic Forces Required to Unbend Eyelid

In the manufacturing process discussed earlier, the device is curled by internal forces leading to a tip deflection δ as depicted in Figure 3. The reactive force R is the force necessary to annihilate the deflection (i.e., to flatten or uncurl the device, see [5]). Here R is defined as

$$R = \frac{48EI}{EL^3}\rho\left(1 - \sqrt{1 - \left(\frac{L}{\rho}\right)^2}\right) \tag{26}$$

(see Young [6]). In a parallel plate capacitor, the electrostatic force F between the plates is given by

$$F = \frac{1}{2}\frac{\epsilon A V^2}{d^2} \tag{27}$$

where d is the distance between the capacitor plates, ϵ is the dielectric constant, A is area, and V is applied voltage. This can be modified to apply to the case where the top plate is curved. Similarly, we can look at the electrostatic force exerted upon the actuator arm.

$$\mathcal{F} = \int_0^L \frac{1}{2}\frac{\epsilon A V^2}{[d + \delta(l)]^2} dl \tag{28}$$

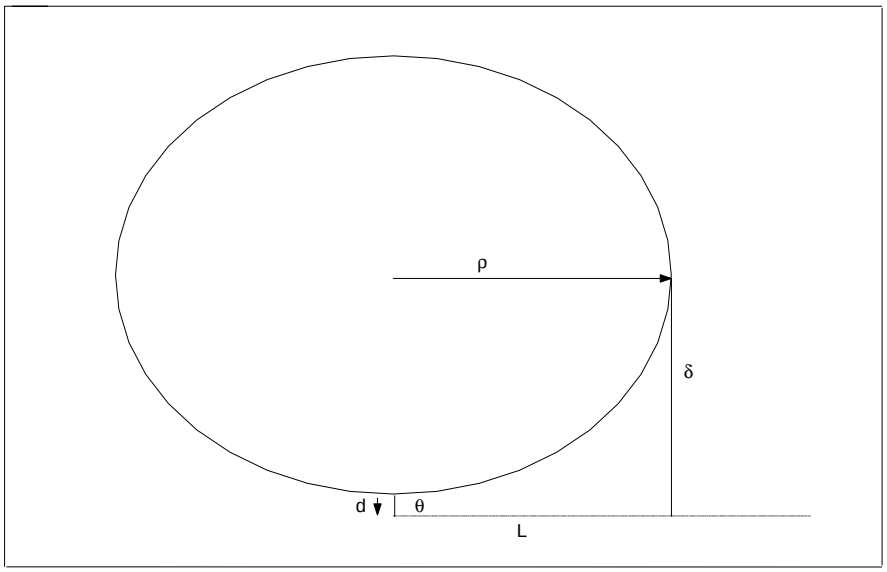

Figure 3: Geometry used to visualize the motion of the film.

where L is the length corresponding to Figure 2 and

$$\delta(l) = \rho \left[1 - \sqrt{1 - \left(\frac{l}{\rho} \right)^2} \right]. \tag{29}$$

Setting $F = R$ yields the relation

$$V = \left[\frac{96EI}{5L^3 \epsilon A} \frac{\rho \left(1 - \sqrt{1 - \left(\frac{L}{\rho} \right)^2} \right)}{\int_0^L \frac{1}{[d+\delta(l)^2]} dl} \right]^{\left(\frac{1}{2}\right)} \tag{30}$$

specifying the voltage required to actuate the device.

3.1 Computation of an Equivalent EI

The equivalent flexural beam strength EI is computed in order to calculate the reactive force and therefore the voltage. In this study, we calculate EI using an equivalent width technique.

First, a cross section of the beam width w is considered in Figure 4. In general, each section has a different Young's modulus (E=stress/strain). One of the materials is chosen as the assumed material (with Young's Modulus E_a). This material maintains the width of the cross-section. The widths of the other materials are given by $w + E_i/E_a$ where E_i is the Young's modulus of the material in question. This leads to a cross section like the one in Figure 5 in which the entire beam consists of the assumed material.

Secondly, the centroid ($\bar{y}$) must be located using the relation

$$\bar{y}_n = \frac{\sum_{i=1}^{n} A_i' t_i h_i}{\sum_{i=1}^{n} A_i'} \tag{31}$$

where $A_i^{'}$ is the area of the modified beam section, h_i is the height of the center of the i^{th} beam section, t denotes thickness of the material, and n is the number of layers.

Finally, the inertial moment ($I^{'}$) for the centroidal axis must be determined. This can be acquired from

$$I' = \sum_{i=1}^{n} \frac{w_i' \left(t_i^3 \right)}{12} + A_i' \left(h_i - \bar{y} \right)^2 \tag{32}$$

where w' is the width of the modified beam section. The equivalent flexural beam strength is given by $EI = E_a I'$.

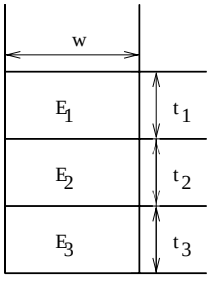

Figure 4: Side view of the individual layers given respective Young's moduli E_i, thicknesses t_i and lengths w.

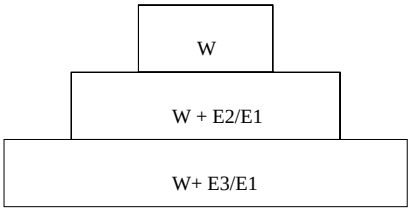

Figure 5: Side-view depicting increasing widths due to addition of the ratio of the Young's moduli.

4 Model Validation

With a varying array of MEMS, we initially consider trends involving this model rather than to analyze specific cases. In the two and three-layer cases, we examine varying aspects which are made easier to understand due to the restriction of fewer layers. In the five-layer case we sought to look at trends by examining computed results to determine if our model was giving desired results for varying a_i.

4.1 Computation of ρ For Two-Layer Case

Using the data provided by MCNC that was known or physically observed, the computation of ρ using the model were computed. Experiments were conducted by varying the top layer of the multilayered strip. This information was among the most coveted in that the initial curvature can be optimized for minimum voltage and still be useful. The two-layer case seemed most reasonable to view this change.

Figure 6 demonstrates the variation of ρ with thickness of the top layer of the multilayered strip. The model used to compute the phenomena is based on a modified form of Judy [4]. Notice that the figure confirms that as the top layer of the polyimide becomes thicker, the radius of curvature increases. This reinforces the idea that not only does the top-layer work against the curvature but it also lessens resistance against the electrical forces wishing to bring the film to contact with the fixed layer on the substrate.

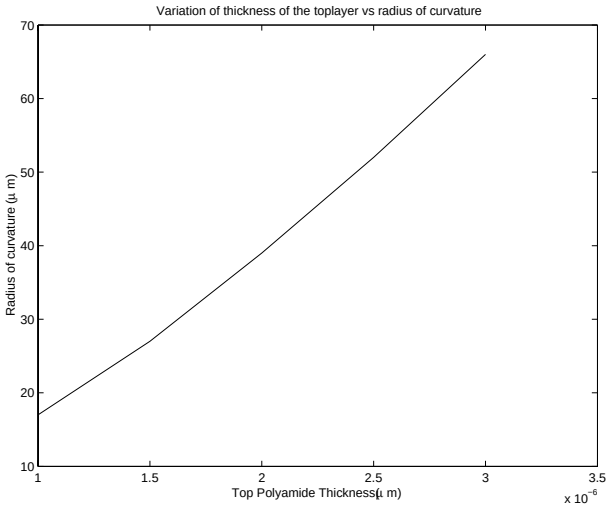

Figure 6: Dependence of the radius of curvature on the thickness of the top polyimide layer.

Thickness (a_3)	Measured	Calculated
5.00e-08 m	45μ m	4.5021e-05 m
4.50e-07 m	120μ m	1.1994e-04 m
8.00e-07 m	250μ m	2.5689e-04 m

Table 1: Computed and measured material dimensions.

4.2 Computation of ρ versus Temperature for Three-Layer Case

An investigation of the relationship between change in temperature in the cooling processes of the polyimide versus ρ was also desired. When our computations were completed, we noted that for greater temperature changes during the cooling of the polyimide, the radius of curvature of the film decreases rapidly. Once again we aimed for the trends of the model. In Figure 7, we present the model predictions which we see agree to within a factor of ten.

4.3 Computation of ρ for Five-Layer Case

We were left with a nonlinear system of equations that we had to solve for ρ. The line search Newton's Method (which converges quadratically provided a reasonably accurate starting point) yielded physically reasonable parameters as summarized in Table 1. Notice that the thicknesses of the layer a_3 increase according to the table. In actual laboratory measurements, the film was shown to have radii of 45, 120 and 250 μm. Hence the model exhibits approximately .000467, .0005, and 2.8 percent relative errors.

4.4 Computation of $E(V)$

The computation of $E(V)$ is little more than an integral which may or may not be difficult to solve depending upon $\delta(l)$ given ρ, EI, and L. Experiments were conducted to test the model for the variations of voltage against both top-layer thickness and radius of curvature.

In the two layer case, top-layer thickness was varied in order to see how the voltage varied. According to Figure 8, as the thickness of the top layer increases the voltage drops. From Figure 9, it was determined that as

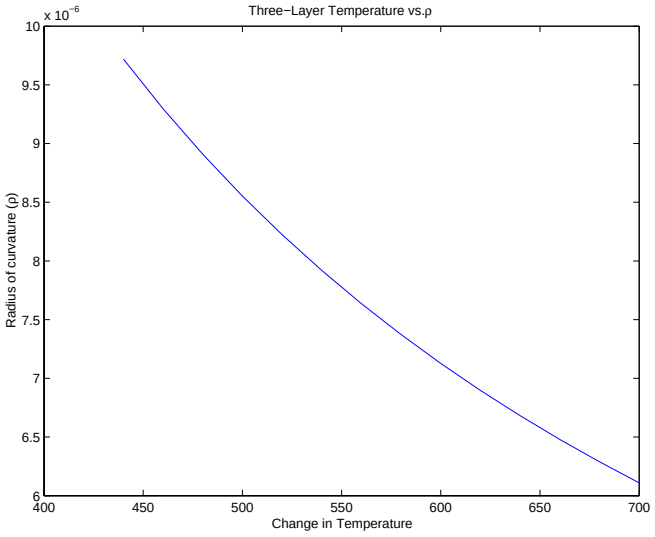

Figure 7: Decrease in the radius of curvature as a function of temperature.

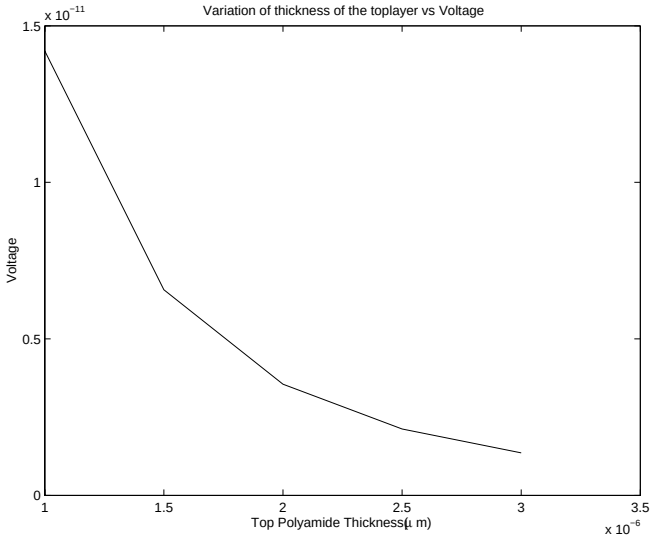

Figure 8: Decrease in the voltage required to lower the cantilever as a function of the thickness of the top polyimide layer.

the radius of curvature increases, the voltage required to actuate the device decreases. As the radius of the arm increases, the distance to the substrate is lowered. If one recalls, due to (27), the electrostatic force between the two plates increases and the voltage required goes to zero according to (30).

The three-layer case was the only one modeled in this situation as opposed to the five-layer case. It determined was that the five and three-layer cases were similar as far as conductivity. The extra two layers were other metal conductors surrounding the gold. However it was noted that their conductivity was similar to that of the gold and therefore should simply be treated as one-layer.

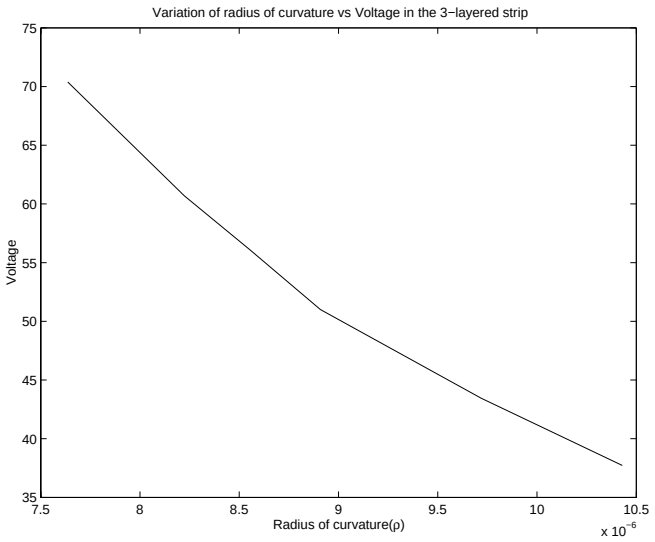

Figure 9: Voltage required to actuate the lever arm as a function of the radius of curvature.

5 Conclusion

The first goal of this investigation was to accurately compute the forces which cause the film (two, three, or five-layers) to bend. Using a combination of models, we constructed systems of equations describing these curvatures that allow us to describe the radii of the structure for other given factors. Numerically, it was shown that the behavior of our model was qualitatively similar to the results gathered in the laboratory. This was a necessary result to complete the second goal.

The second goal of this paper was to model the electric forces acting upon the MEMS when attempting to actuate the device. Modeling the voltage over the length of the structure was an definitely an area of interest. The numerical results from our model further validated its accuracy by giving us the trends that analysis of our voltage modeling equations led us to believe would occur.

Acknowledgements

The Industrial Mathematics Modeling Workshop was supported by Statistical and Applied Mathematical Sciences Institute (SAMSI) with additional support provided by the Center for Research in Scientific Computation (CRSC) and the Department of Mathematics, North Carolina State University.

References

[1] M. Capozzoli, J. Gopalakrishnan, K. Hogan, J. Massad, T. Tokarchik, S. Wilmarth, H.T. Banks, K.M. Mossi and R.C. Smith, "Modeling aspects concerning THUNDER actuators," Proceedings of the SPIE, Smart Structures and Materials 1999, Volume 3667, pp. 719-727, 1999.

[2] A.K. Chinthakindi and P.A. Kohl, "Electrostatic actuators with intrinsic stress gradient," *Journal of the Electrochemical Society,* 149(8), H139-H145, 2002.

[3] G. Daspit, C. Martin, J-H. Pyo, C. Smith, H. To, K.M. Furati, Z. Ounaies and R.C. Smith, "Model development for piezoelectric polymer unimorphs," Proceedings of the SPIE, Smart Structures and Materials 2002, Volume 4693, pp. 514-524, 2002.

[4] M.W. Judy, Y-H. Cho, R.T. Howe and A.P. Pisano, "Self-adjusting microstructure (SAMS)", IEEE, pp. 51-56, 1991.

[5] S. Timoshenko "Analysis of bi-metal thermostats," *Journal of the Optical Society of America*, 11, 233-255, 1925.

[6] R.J. Roark and W.C. Young, *Formulas for Stress and Strain*, McGraw-Hill, New York, 1975.